EFFECTS ON SPACECRAFT RADIOMETRIC DATA AT SUPERIOR SOLAR CONJUNCTION

Trevor Morley(1) **and Frank Budnik**(1)

European Space Operations Centre (ESOC), Robert-Bosch-Strasse 5, 64293 Darmstadt, Germany
(1)*ESA/ESOC, E-mail: <first name>.<last name>@esa.int*

Abstract

During 2006, three ESA interplanetary spacecraft, Rosetta, Mars Express (MEX) and Venus Express (VEX), passed through superior solar conjunction.

For all three spacecraft, the noise in the post-fit range-rate residuals from the orbit determination was analysed. At small Sun-Earth-Probe (SEP) angles the level was almost two orders of magnitude higher than normal. The main objective was to characterise the Doppler (range-rate) noise as a function of SEP angle. At least then the range-rate data can be appropriately weighted within the orbit determination so that the solution uncertainties are realistic.

For VEX, some intervals of particularly noisy Doppler data could be correlated with unusual solar activity.

For Rosetta, the biases in the range data residuals were analysed with the aim of improving the model used for calibrating the signal delay due to the solar plasma. The model, which originally had fixed coefficients, was adjusted to achieve better fits to the data. Even the relatively small Doppler biases were well represented.

Using the improved model, the electron density at 20 solar radii was compared with earlier results obtained by radio science studies using Voyager 2 and Ulysses radiometric data. There is some evidence for a dependency of the density on the phase within the 11 years solar cycle.

1. Introduction

Rosetta, in heliocentric cruise, passed through superior solar conjunction in April 2006. For both MEX and VEX, in orbit around their planet namesakes, the conjunctions occurred in late October 2006, within 5 days of each other. For Rosetta and VEX it was the first experience of superior conjunction and for MEX the second, the first having occurred in September 2004.

During such conjunctions the signals to and from the spacecraft pass through the solar corona surrounding the Sun. The free electrons in the plasma cause a group delay on ranging measurements and a phase advance on Doppler measurements, just as the electron density in the Earth's ionosphere does. The magnitudes of these effects are inversely proportional to the square of the signal frequency - X-band for all three of the ESA missions. Since the electron density increases with decreasing distance from the Sun, following, at least approximately, an inverse square law, the effects on the radiometric data increase as the SEP angle diminishes.

As is well known, the main effect on Doppler measurements is a substantial increase in the data noise. For SEP angles below about 1°, a variable bias also becomes significant. In contrast, range data noise levels are hardly affected but the additional variable bias on the measurements can easily reach several hundred metres.

In the absence of simultaneous two-way dual-frequency links, the Doppler noise cannot be mitigated and the degree of success in calibrating out the range bias depends upon the fidelity of the solar plasma modelling. Thus, superior solar conjunctions are times when orbit determination accuracy can be severely degraded.

Under normal circumstances, the MEX and VEX orbits are determined using only Doppler data - the addition of range data leads to insignificant improvements in accuracy. Nevertheless, ranging measurements are routinely acquired. The range residuals are computed mainly for purposes of analysing errors in the ephemerides of Mars and Venus. Over solar conjunction periods, resolving the signatures of the residuals between the contribution of such errors and the solar plasma effects is not straightforward so only the Doppler noise was investigated for these two missions.

With favourable conditions, the noise standard deviation on 2-way range-rate measurements, compressed to 1-minute count times, is below 0.1 mm/s in data acquired by ESA's 35 m antennas of the deep space stations at New Norcia (NNO) in Western Australia and Cebreros (CEB) in Spain and the stations of the NASA Deep Space Network (DSN) complexes. The observed noise levels during the MEX and VEX solar conjunctions are described in section 2 and the results compared in section 3. In section 4, the MEX results are compared with those of the 2004 solar conjunction.

The noise seen on both the range-rate and range measurements during the Rosetta solar conjunction are described in section 5.

For a spacecraft like Rosetta, in heliocentric orbit, range data in addition to Doppler data are indispensable for obtaining adequately accurate orbit solutions. During the solar conjunction operations it was clear that the model then being used to calibrate the solar plasma effects,

especially on the range, was predicting much larger data biases than were being observed. Sections 6 and 7 explain how the model, which originally had fixed coefficients, was adjusted and improved to achieve much better fits to the data, including the relatively small Doppler biases.

Using the improved model, the electron density radial profile was analysed and the estimated density at 20 solar radii is compared in section 8 with earlier results obtained by radio science studies using Voyager 2 and Ulysses radiometric data.

2. MEX and VEX Solar Conjunctions

Seen from Earth, both spacecraft passed north of the Sun, MEX moving across the sky from approximately east to west and VEX moving from west to east (Fig. 1). On 25 October, the angular separation between the two spacecraft was less than 1 ° .

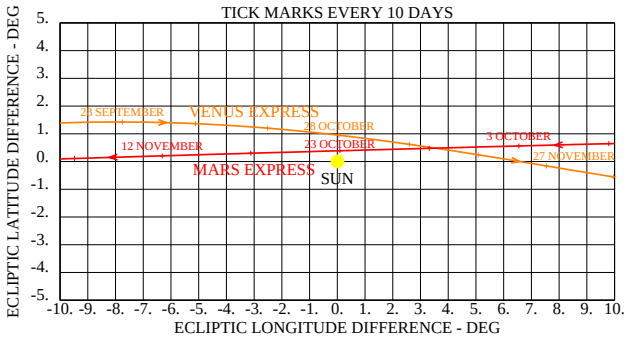

Fig. 1. MEX and VEX solar conjunctions in 2006

2.1 MEX solar conjunction

The MEX SEP angle remained below 10 ° for two months centred on the day of the minimum SEP angle. This minimum was 0.39 ° (1.6 solar radii) and occurred at 08:39 UTC on 23 October when the spacecraft's geocentric distance was 2.59 AU.

Over the two months, Doppler data were acquired during 44 passes from NNO, supplemented with 7 passes from CEB, all close to the middle of the conjunction, and 43 passes using almost all the large antennas at the NASA/DSN complexes at Goldstone and Madrid. The 70 m DSS 63 antenna at Madrid was not available due to major repairs.

Fig. 2 shows the post-fit, 2-way, 60 s count-interval range-rate residuals; they correspond to 15572 data points. Routine MEX orbit determinations were then based on tracking arcs of 5 - 7 days duration, corresponding to approximately 18 - 25 orbital revolutions, with a typical overlap of 2 days between successive arcs. So Fig. 2 is a concatenation from several orbit solutions. Residuals in each overlapping interval were actually taken from the earlier solution but the residuals hardly differ in the overlaps between successive solutions.

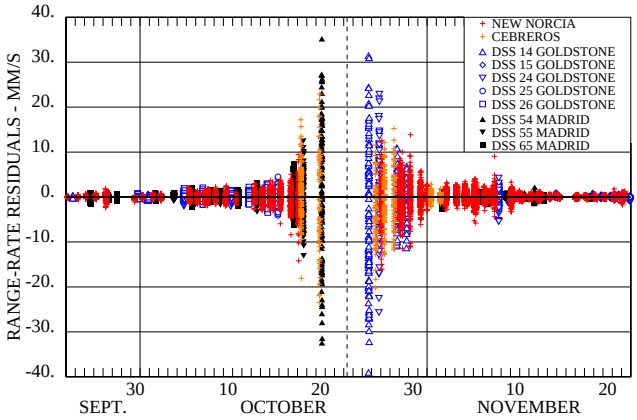

Fig. 2. MEX post-fit 2-way range-rate residuals

Within two days from the middle of the conjunction, denoted by the dashed vertical line, no tracking was scheduled except for a DSS 24 Goldstone pass late on 24 October. At the middle of the pass the SEP angle was 0.62 ° and the data are extremely noisy. For scaling reasons, these residuals, whose maximum value was almost 200 mm/s, are not shown in Fig. 2[1]. The root mean square (rms) of these residuals is 57.8 mm/s. There is also a distinctly positive mean value or bias that is to be expected for data acquired at low SEP angles after the time of minimum SEP angle, when no solar plasma correction model is applied - see section 7.1.

In Fig. 3, the rms residual values for each individual pass are plotted against the SEP angle at the mid-point times of each pass. A negative value for the angle denotes ingress into the solar conjunction.

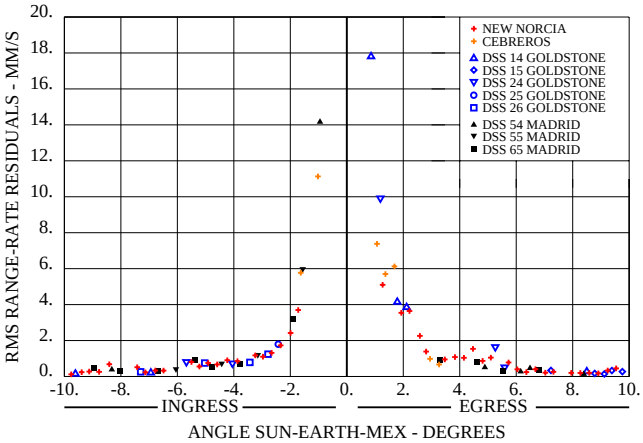

Fig. 3. MEX rms 2-way range-rate residuals

These results show that, although there are fluctuations in the Doppler noise level from day to day, there is a relatively steady increase in noise as the SEP angle diminishes. From an SEP angle of about 3 ° downwards, there

1. 3 residuals, slightly more negative than -40 mm/s, from the DSS 14 pass on 25 October, are also not shown.

is a sharp rise in the rate of noise increase. As expected, the plots also show that there is no station dependency of the Doppler noise.

At the extremes, i.e. one month from the middle of the solar conjunction when the SEP angle was approaching 10°, the rms range-rate noise is only marginally higher than average values measured when MEX is far away from the Sun.

2.2 VEX solar conjunction

VEX passed through solar conjunction more slowly than MEX so that the SEP angle was continuously less than 8° over the two months centred on the day of the minimum SEP angle. This minimum was 0.95° (3.8 solar radii) and occurred at 21:21 UTC on 27 October when the spacecraft's geocentric distance was 1.72 AU.

Over the two months, Doppler data were acquired during 60 CEB passes, supplemented with 18 NASA/DSN passes, all but two at Canberra. Originally, it was foreseen that all the Canberra passes, scheduled for radio science purposes, would use the 70 m DSS 43 antenna but, in the event, 2 passes were with DSS 45 and one pass with DSS 34, both 34 m antennas.

Fig. 4 shows the post-fit, 2-way, 60 s count-interval range-rate residuals; they correspond to 23485 data points. Routine VEX orbit determinations are based on tracking arcs of 10 days duration, corresponding to 10 orbital revolutions, with an overlap of 3 days between successive arcs. So Fig. 4 is a concatenation from several orbit solutions.

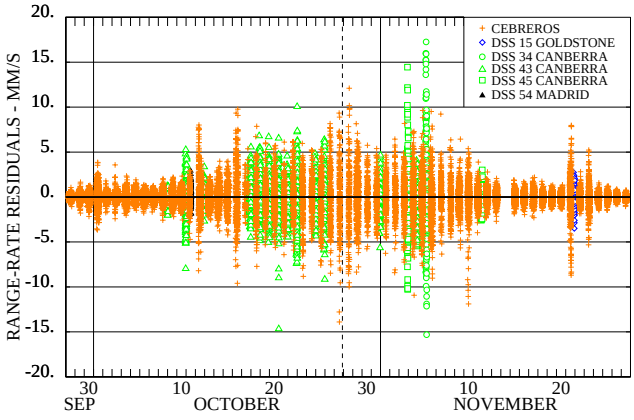

Fig. 4. VEX post-fit 2-way range-rate residuals

Fig. 5 shows the rms residual values for each individual pass plotted against SEP angle. Compared with the MEX results, Fig. 5 shows larger day-to-day fluctuations in the range-rate noise levels. Also, there is no apparent sharp rise below an SEP angle of about 3°.

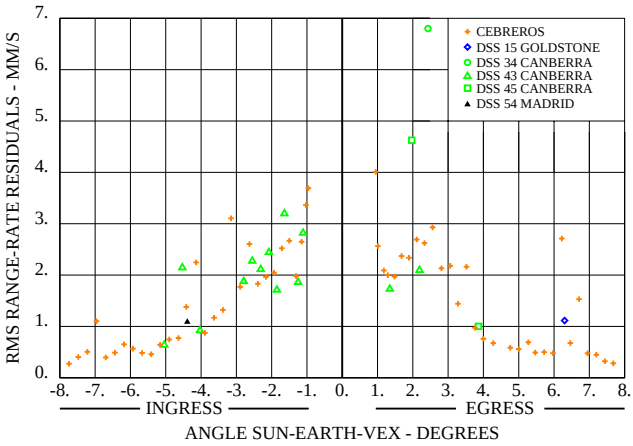

Fig. 5. VEX rms 2-way range-rate residuals

At the extremes of the solar conjunction period, on 28 September and 27 November, the rms range-rate residuals were 0.27 and 0.28 mm/s respectively. These values are still about five times higher than the best ones achieved when the spacecraft direction is well away from the Sun. Therefore, as concerns an impact on orbit determination accuracy, the VEX solar conjunction extended over a duration of longer than two months.

2.3 VEX Doppler data noise and solar activity

Within the egress interval, the noise levels over some individual passes or during parts of individual passes were discordantly high. For example, the magnitude of residuals in the early part of the 03 November DSS 45 pass reached 40 mm/s and in the early part of the 05 November DSS 34 pass reached 80 mm/s. These really bad quality data were deleted but the rms values of the remaining residuals were still unexpectedly high. During 1 - 2 hour intervals in the middle of the CEB pass on 06 November and at the end of the CEB pass on 07 November, residuals as high as 60 mm/s appeared. In these cases, after deletion of the data from the affected intervals, the rms values of the remaining residuals were not abnormally high.

Two more examples occurred during the 21 & 23 November CEB passes. In these cases, no data were deleted. On 21 November, the particularly bad quality data appeared over a one hour interval close to but before the end of the pass. On 23 November they appeared at the start of the pass.

After the official end of the solar conjunction phase further such examples occurred during CEB passes, on 01, 05 & 06 December. For the last two passes the noise increase was quite abrupt at shortly after 13:00 UTC on 05 December and remained continuously high through to the end of the 06 December pass. In this particular case there is quite some evidence that a solar flare was the cause. For instance, on 05 and 07 December, unusu-

ally high numbers of EDAC (error detection and correction) events were registered within the VEX data management system.

An abnormally high number of EDAC events did not occur on the earlier occasions when noisy Doppler data were acquired. Nevertheless, it may be that unusual solar activity was the cause for at least some of the noisy passes. To be a plausible explanation, the activity would have to have been concentrated on the eastern side of the Sun otherwise the MEX Doppler data should also have been adversely affected. Table 1 gives a summary of the occasions with noisy VEX Doppler data, including remarks on solar activity. This information was taken from the spaceweather.com web site [1].

Table 1: VEX passes with unusually high Doppler noise

Date	Station	Interval	Max. residual (mm/s)	Solar activity
11/03	DSS 45	Whole pass	40	Large sunspot forming on far side of Sun in early November
11/05	DSS 34	Whole pass	80	
11/06	CEB	1-2 hours in middle	60	Eruption from sunspot just behind the eastern limb
11/07	CEB	1-2 hours at end	60	
11/21	CEB	1 hour near end	8	On 20 November, coronal mass ejection from far side near eastern limb
11/23	CEB	1 hour at start	6	
12/01	CEB	1st half of pass	5	Big prominence at eastern limb
12/05	CEB	2nd half of pass	5	On 05 December, major flare from large sunspot near the eastern limb
12/06	CEB	Whole pass	3	

3. Comparison of MEX and VEX Results

The 1-way signal path to MEX was 0.87 AU longer than that to VEX. However, the electron density in the solar plasma follows (at least approximately) an inverse square law with distance from the Sun. This means that the total electron content along the path from Earth to Mars is only marginally higher than along the path from Earth to Venus, for equivalent SEP angles. Therefore, the influence on the MEX and VEX Doppler noise would be expected to be very similar.

By and large, this is confirmed by Fig. 6 in which the rms residual values have been plotted against SEP angle. A differentiation is made between east and west of the Sun so, for VEX, the signs of the SEP angles have been reversed from those shown in Fig. 5.

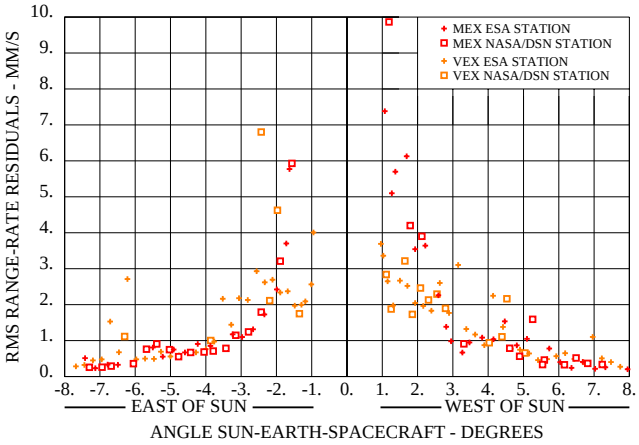

Fig. 6. MEX and VEX rms 2-way range-rate residuals

The only distinct difference is west of the Sun at SEP angles between 1° and 2° when the MEX residuals are significantly larger. From Fig. 1 it can be seen that VEX crossed this region on round about 23 October and MEX five days later round about 28 October. Thus, the results could be due to a change in the plasma characteristics during the five days or due to the different relative location of VEX, north-west of the Sun, whereas MEX was closer to due west, or a combination of both causes.

4. Comparison of MEX Results from 2004 and 2006

Fig. 7 shows the 2-way range-rate rms values plotted against SEP angle for both the 2004 and 2006 MEX solar conjunctions. Ignoring the occasional, discordantly high noise level during the 2004 conjunction, the variation with SEP angle is similar for both conjunctions except during the ingress period between about 4.5° and 2° when the noise during the 2004 conjunction was continuously higher with more marked day to day fluctuations.

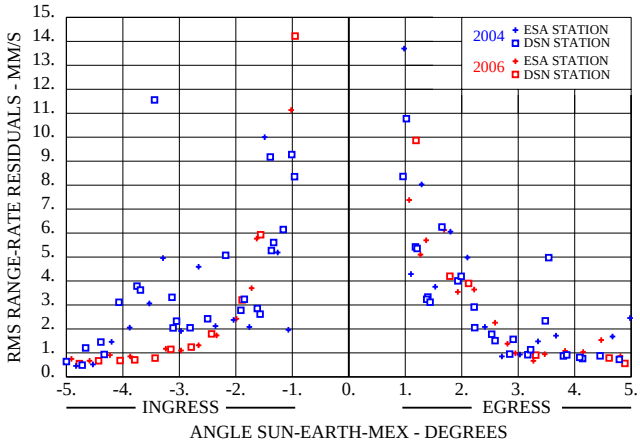

Fig. 7. MEX rms range-rate residuals in 2004 and 2006

5. Rosetta Solar Conjunction

The Rosetta SEP angle remained below 10° for two

months between 16 March and 15 May 2006. The minimum SEP angle of 0.54° (2.2 solar radii) occurred in the afternoon of 12 April (Fig. 8) when the spacecraft's geocentric distance was 2.58 AU.

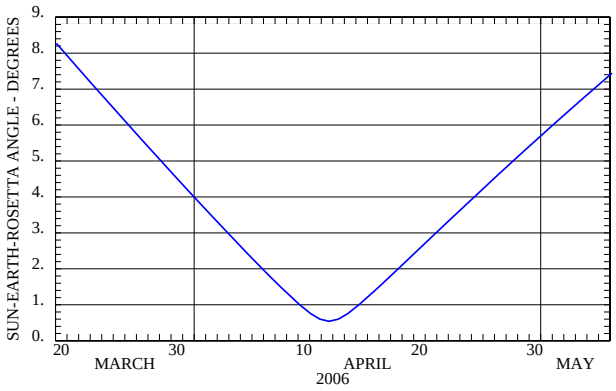

Fig. 7. Rosetta SEP angle

For the whole period of the solar conjunction, the sole ground station supporting the mission was NNO. Between 4 - 28 April inclusive, Rosetta was tracked every day for typically up to 4 hours except on 9 April when there was no pass. Outside of this interval, but within the period when the SEP angle was less than 10°, Rosetta was tracked on about half the available daily opportunities.

5.1 Rosetta range-rate noise

Fig. 8 shows the post-fit, 2-way, 60 s count interval range-rate residuals over almost two months, from 15 March until 11 May; they correspond to 7616 data points. At the start of this period the SEP angle was 10° and at the end 9°. The actual data arc used for the orbit determination was much longer, with a start date of 02 December 2005, but the residuals before the solar conjunction are not of interest here.

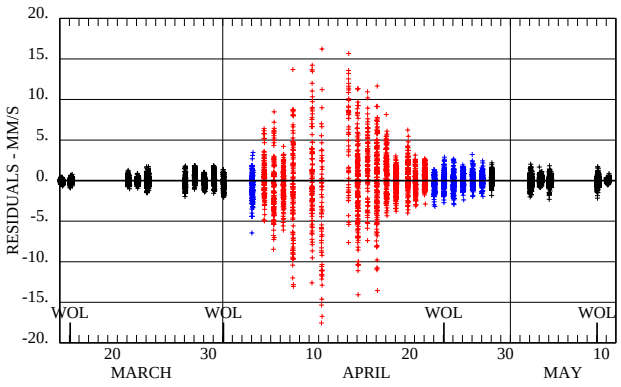

Fig. 8. Rosetta NNO post-fit 2-way range-rate residuals

On 12 & 13 April, apart from there being many outliers, the residuals were obviously biased by about +11 m/s. This is likely to have been due to an inconsistent configuration at the station in which the reference frequency was wrong by approximately 300 Hz. Since this is not known for certain, the range-rate data on these two days had to be discarded.

There were a few outliers on 11 April that were also deleted, but the majority of the data on that day could be used. The successful acquisition of Doppler data on 11 & 14 April provided usable data corresponding to a SEP angle down to 0.70°.

As indicated in Fig. 8, there were four reaction wheel momentum offloadings (WOLs) during the solar conjunction, but outside the interval of smallest SEP angles. Nominally, the thrusters are balanced and routine calibrations show that the orbit disturbances due to WOLs are minimal, with a typical ΔV of a small fraction of a mm/s.

Within the orbit determination, for the residuals shown in black, the corresponding data were weighted with the usual, conservative 1σ noise level assumed to be 0.2 mm/s. For the data in blue this was increased to 2 mm/s and the data in red were totally deweighted so that they had no influence on the orbit solution.

The general increase in range-rate noise with decreasing SEP angle is the obvious feature in Fig. 8. On 11 April, the residual standard deviation is 7.0 mm/s and on 14 April is 5.6 mm/s. It may be noted that on these two days the mean values of the residuals are distinctly non-zero; negative on 11 April and positive on 14 April. This is further discussed in section 7.1.

On 15 March and 11 May, the rms range-rate residuals were about double typical values well away from conjunction. This shows that the solar plasma still had a significant influence on Doppler data noise at SEP angles of the order of 10°, and in this case one month away from the middle of the solar conjunction.

5.2 Rosetta range noise

Lock of the ranging signal could not be achieved at the smallest SEP angles during the four days from 11 - 14 April inclusive. Ranging data were successfully acquired for all the other tracking passes and notably on 10 & 15 April when the minimum SEP angle on both days was 0.95°.

Mismodelling of systematic influences, particularly those affecting range, typically lead to residuals with near zero overall mean but with different non-zero values from pass to pass. Except at very small SEP angles, the range residual bias over the course of an individual pass remains quite constant. Then the standard deviation (rather than rms) of the residuals over a single pass reflects the measurement noise. Alternatively, within the orbit determination, a range bias per station and per pass can be estimated. This is the standard practice for routine orbit determinations and necessarily causes the value of the mean post-fit residual for each pass to be zero unless

the bias is constrained by setting a low *a priori* uncertainty.

In order to examine the noise on the range data, an orbit determination run was made with a range bias estimated per pass. At relatively small SEP angles, due mainly to shortcomings in the solar plasma model, the biases can be much larger than normal. To ensure that the *a posteriori* residuals over each pass would have near zero mean values, the *a priori* 1σ uncertainty on the 1-way range bias was set to 100 m.

From the raw range measurements, individual data points, without smoothing, were extracted every 20 minutes for inclusion in the orbit determination. The resulting 2-way range residuals are plotted in Fig. 9.

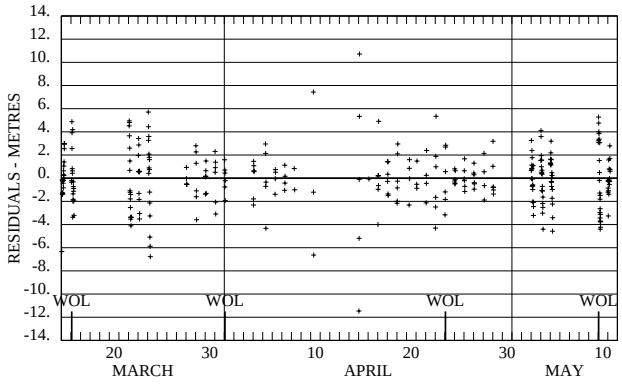

Fig. 9. Rosetta NNO post-fit 2-way range residuals
Range bias per pass removed

Except, apparently, for the residuals on 10 & 15 April, there is no discernible increase in range noise with decreasing SEP angle. But at very small SEP angles the bias due to the plasma varies significantly with even tiny increments in the SEP angle so the bias is not close to constant over a pass. For example, over the 75 minutes covered by the data from 15 April, the SEP angle increased by about $0.01°$ and the five residuals are located on a downward sloping line. Therefore, the overall result is that the noise on the range measurements is hardly affected by how close the signal passes by the Sun.

6. Solar Corona Model

The solar corona model, that was used to correct the radiometric data for the effects of the electron content within the plasma, is based upon the following profile for the electron density, N_e:

$$N_e = \frac{A}{r^6} + \frac{B}{r^{2+\varepsilon}} \quad \text{electrons cm}^{-3} \qquad (1)$$

where r is the solar distance expressed in units of the solar radius (~696000 km), A and B are constant coefficients and ε is a small positive fraction.

The corona delay, $\Delta\tau$ (μs), is computed from:

$$\Delta\tau = \frac{40.3}{cf^2}\int_{P_1}^{P_2} N_e ds \qquad (2)$$

where c is the speed of light (km s^{-1}), f is the frequency (MHz) of the radio carrier signal and the integration is carried out over the linear distance (km) from point P_1 to point P_2 in space. The integration is performed separately for the up- and downlink paths between the ground station and spacecraft. Details on how the integral can be evaluated are given in [2].

Since integrated Doppler is the same as range difference, the correction to range-rate data is found by differencing the computed delays at the start and end of the count interval, changing the sign and dividing by the count interval.

From analysis of Mariner-6 data, Muhleman *et al*. [3] made the following estimates with 1σ uncertainties:

$$A = (0.69 \pm 0.85)\times 10^8$$

$$B = (0.54 \pm 0.56)\times 10^6$$

$$\varepsilon = 0.05 \pm 0.24 .$$

Mariner-7 did not pass near enough to the Sun to be sensitive to the A term so Muhleman *et al*. adopted the value of A from previous studies and estimated the other two parameters:

$$A = (1.3 \pm 0.9)\times 10^8$$

$$B = (0.66 \pm 0.53)\times 10^6$$

$$\varepsilon = 0.08 \pm 0.23 .$$

The Mariner solar conjunctions occurred in 1970 at a period of solar maximum activity [4]. For all values of r for which data were collected, the electron density was found to be higher for Mariner-7. The 1σ uncertainties on the estimates, though, are of the same order of magnitude as the estimates themselves. Both pairs of estimates for B and ε give an electron density at 1 AU (215 solar radii), i.e. at the Earth, of about 9 electrons cm^{-3}.

For processing radar and Mariner-9 data within the effort to set up the JPL DE102 planetary ephemerides [5], the same basic model was used but with a different combination of parameter values, namely:

$$A = 1.3\times 10^8$$

$$B = 0.5\times 10^6$$

$$\varepsilon = 0.0.$$

With one minor difference, this model was implemented when ESOC's orbit determination software was set up and had remained unchanged ever since. The electron density profile is assumed to be given by:

$$N_e = K_p\left(\frac{1.3\times10^8}{r^6} + \frac{0.5\times10^6}{r^2}\right) \quad \text{electrons cm}^{-3} \quad (3)$$

where K_p is a coefficient or scaling factor, with a nominal value of unity, that could be treated as an uncertain parameter and, if desired, estimated within the orbit determination. With this version of the model, the contribution of the two terms to the density is the same at 4.02 solar radii.

6.1 Range corrections from solar corona model

For 2-way X-band data, Table 2 gives the increase in the length of the 2-way signal path computed from the nominal model (K_p = 1) for discrete SEP angles between 10° and 180° and for spacecraft geocentric distances between 0.5 AU and 3.0 AU.

Table 2: Solar corona range corrections (metres)

SEP Angle	Geocentric Distance (AU)					
	0.5	1.0	1.5	2.0	2.5	3.0
10°	2.2	19.0	33.8	35.8	36.5	36.8
20°	2.0	9.1	14.6	16.1	16.7	17.1
30°	1.8	5.8	8.7	9.8	10.3	10.6
60°	1.3	2.7	3.5	4.0	4.3	4.5
90°	1.0	1.7	2.2	2.5	2.6	2.8
180°	0.7	1.1	1.3	1.5	1.6	1.7

For an SEP angle above 30°, the correction does not exceed 10 m. Even at an SEP angle of 10°, the correction is less than 40 m. At low SEP angles and above 1.5 AU, the correction is only weakly dependent upon the geocentric distance.

Outside of solar conjunction periods, because the range correction is relatively small and quite uncertain (but must be virtually constant over the duration of a single pass) and, above all, because the range-rate correction is negligible, it is the usual practice not to apply explicit corrections due to the solar corona within the orbit determination. Instead, the effect on the range measurements is absorbed as one of the contributions to the overall range bias that is estimated for each station pass.

6.2 Nominal solar corona model applied to Rosetta

The contribution to the corona delay (equation (2)) from the r^{-6} term in equation (3) is insignificant when the SEP angle is above 2°. Also, the contributions from this and the r^{-2} term are the same at an SEP angle of 0.85°. Since no range data were acquired below an SEP angle of 0.95°, the r^{-2} term is the dominant one for all the Rosetta range corrections.

It became obvious from the results of various orbit determination runs that the apparent range increase due to the solar corona was substantially less than that given by the nominal model.

In one orbit determination run with a fairly standard set-up and with no data excluded by being zero-weighted, the coefficient K_p was included in the vector of solve-for parameters. The outcome was an estimate of K_p = 0.18. However, the characteristics of the *a posteriori* residuals were much less random than usual and thus the result lacked credibility.

7. Adjusted Solar Corona Model

Variations in estimates for K_p using different fitting techniques suggested that the relative contributions of the two terms in the nominal model could not be applicable to the case of the Rosetta solar conjunction. Consequently, the orbit determination software was modified, omitting K_p but including the capability to estimate separately each of the coefficients A and B.

Several runs were made with the amended orbit determination using different set-ups. The results presented here are taken from a solution using a tracking data arc from 15 March to 11 May inclusive. The assumed 1σ noise on the range data was 5 m (the standard weighting) for the entire arc. For the Doppler data, the assumed 1σ noise was somewhat optimistic, 2 mm/s for the interval 04 - 29 April inclusive, and the standard value of 0.2 mm/s outside of this interval.

Range biases on a per station per pass basis were estimated but constrained more than usual by setting an *a priori* 1σ uncertainty of only 5m, 1-way. This was done in order to try and avoid the effect of the solar plasma being absorbed into the range bias estimation.

For a similar reason, the *a priori* scale factor correction to the main component of the acceleration due to solar radiation pressure (the percentage correction to the value from the nominal model), along the Sun - spacecraft direction, was set to +7.5% with a constrained 1σ uncertainty of just 1%. These quantities are consistent with the mean value and its variation estimated throughout the Rosetta mission before and after the solar conjunction. Without the constrained uncertainty, the *a posteriori* estimate in other runs was as high as 16% which is unrealistic.

The three cartesian, acceleration components of each of the 4 WOLs were estimated in the normal way.

Finally, the *a priori* estimates for A and B were taken from the nominal solar corona model with 1σ uncertainties of 100%, in line with the results from [3].

7.1 Solar corona model estimates and data fit

The model parameter estimates together with their 1σ uncertainties were:

$$A = (0.12 \pm 0.01)\times 10^{8}$$

$$B = (0.41 \pm 0.02)\times 10^{6}.$$

Compared with the nominal model, both coefficients are smaller, A by an order of magnitude and B by 20%. The estimated value for B leads to an electron density at 1 AU of 8.9 electrons cm^{-3}, consistent with the results using the Mariner data.

All the estimates of the WOL components seemed reasonable in that they were small with sizes typical of those seen in routine operations. The *a posteriori* estimate for the solar radiation pressure scale factor was +9.2%.

In order to visualise directly how well the adjusted solar corona model fits the data, the following procedure was adopted. Using the estimates of all the parameters solved-for in the orbit determination, except for the range biases that were set to zero, a pass-through of the data was made, omitting the corrections from the solar corona model. The resulting 2-way range residuals are plotted as crosses in Fig. 10.

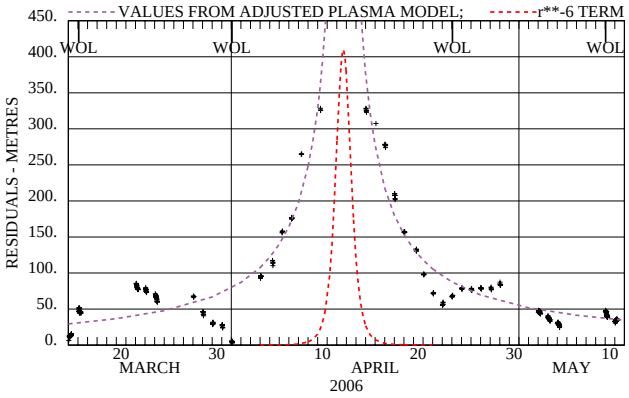

Fig. 10. Rosetta range residuals from pass-through
No corrections from solar corona model

The superimposed, purple dashed line shows the range corrections as computed from the adjusted solar corona model. Overall, the fit appears to be quite good.

Fig. 11 is the analogous plot showing the 2-way range-rate residuals from the pass-through and the corrections from the adjusted model. The obvious biases in the data on the 11 & 14 April are well accounted for. Because of the large ratio, noise-to-bias, on the range-rate data (in contrast to the large ratio, bias-to-noise, on the range data) little more can be said on fit quality except to regret that the data acquired on 12 & 13 April had to be discarded.

With the adjusted plasma model, Fig. 11 shows that the contributions to the range-rate biases on 11 & 14 April from the r^{-6} and r^{-2} terms are about the same. On the other days the contribution from the r^{-6} term is insignificant. Also, Fig. 10 shows that the contribution to the range bias from the r^{-6} term outside the interval 11 - 14 April is insignificant. As no range data were acquired within this interval it must be the case that the estimate for the coefficient A of the r^{-6} term comes essentially from the information content within the range-rate data on 11 & 14 April. This was confirmed by a test that omitted these data: the 1σ uncertainty on the estimate for A increased by a factor of 40. The 1σ uncertainty on the estimate for B also increased substantially, by a factor of 10.

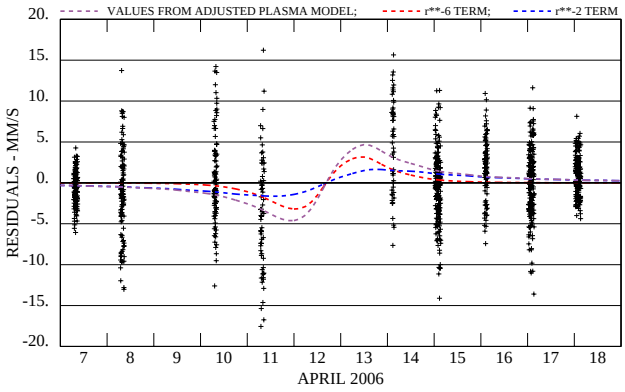

Fig. 11. Rosetta range-rate residuals from pass-through
No corrections from solar corona model

Following a similar argument, it is apparent that the quoted 1σ uncertainty on A of 0.01×10^{8} is optimistic. The assumed 1σ noise on the range-rate data close to the middle of the solar conjunction was set to 2 mm/s but the standard deviation of the residuals are 7.0 mm/s on 11 April and 5.7 mm/s on 14 April. Therefore, a more realistic uncertainty for A is a least 3 - 4 times higher.

8. Comparison with other Electron Density Estimates

Compared with results from the nominal solar corona model, the electron density near the Sun computed from the adjusted model is somewhat lower (~20%) at moderate SEP angles and substantially lower at SEP angles around 1° or smaller. One straightforward explanation could be that the Rosetta solar conjunction occurred at the minimum of the 11 years (on average) solar cycle.

However, a model for the electron density profile that includes a dependency on the phase within the solar cycle is not found in the literature. For example, the model proposed in [6], for low heliospheric latitude and equatorial regions, is:

$$A = 2.21\times 10^{8}$$

$$B = 1.55\times 10^{6}$$

$$\varepsilon = 0.3.$$

For small to moderate SEP angles this gives an electron density even higher than the nominal model within the orbit determination software. In [6] it is claimed that the primary difference between several models postulated

for the electron density profile is the value of ε.

The model described in [2], which is partly based on one derived from Viking measurements in [4], has ε = 0 and there is an additional term dependent upon the latitude relative to the Sun's mean equator of date of the closest approach point to the Sun of the spacecraft signal. But in this model no "nominal" values are given for A and B and nor for the coefficient of the extra term.

The solar corona density distribution was determined during the 1991 solar conjunction of Ulysses [7]. The analysis exploited the range measurements from the dual-frequency (S- and X-band) downlinks that were phase coherent with the S-band uplink. In the same reference, results were also similarly derived from earlier experiments on Voyager 2. During these solar conjunctions the SEP angle did not fall below about 1.3° so the r^{-6} term was ignored.

Table 3 summarises the results that are split between the conjunction ingress (I) and egress (E) phases. Without this split, results are also included from the Viking data [4] and from the nominal and adjusted models of this paper.

Table 3: Electron Density Radial Profile Parameters

Spacecraft	Date	Solar cycle phase	r range (solar radii)		$B(x10^6)$	ε	N_e (r=20) (el. cm^{-3})
Ulysses	Aug 1991	max. +25 months	I	5-33	3.61±0.04	0.54±0.05	1800
			E	5-42	2.26±0.03	0.42±0.05	1600
Voyager 2	Dec 1988	max. -7 months	I	10-85	2.95±0.04	0.08±0.05	5800
			E	14-88	6.94±0.11	0.28±0.05	7500
Voyager 2	Dec 1985	min. -9 months	I	6-38	4.13±0.07	0.63±0.07	1600
			E	7-38	0.52±0.01	–0.06±0.07	1500
Viking	Nov 1976	min.	3-215		N/A	N/A	915
"Nominal Model"	-	-	-		0.5	0 (fixed)	1250
Rosetta	Apr 2006	min.	3-40		0.41±0.02	0 (fixed)	1025

Table 3 shows evidence for an electron density dependence on solar activity. The two lowest estimates at 20 solar radii, equivalent to an SEP angle of 5°, from the Viking and Rosetta conjunctions, occurred at solar minimum. Also, a low value was estimated for B during the egress phase of the Voyager 2 1985 conjunction. In contrast, the highest estimates for the density were made for the Voyager 2 1988 conjunction - the one closest to solar maximum.

There are considerable asymmetries between the ingress and egress phases in the estimates of both B and ε. For the conjunctions of Ulysses and Voyager 2 in 1985, the pairs of values actually yield similar estimates for the electron density on both sides of the Sun at 20 solar radii.

According to [7], the radial profile of electron density is intimately connected to the solar wind's radial velocity profile by the conservation of mass equation. A value $\varepsilon \approx 0$ is to be expected if the solar wind expansion velocity is constant and radially symmetric. A decrease in the density steeper than that given by a r^{-2} law implies significant solar wind acceleration. But if the assumption of spherical symmetry is not valid, i.e. latitudinal and longitudinal variations are present, they too can have a significant effect on the value of ε derived from such radio science experiments.

The wide variation in the estimates of the parameters of the solar corona model makes it clear that no choice of values can provide a reliable, predictive capability for the effects on radiometric data of an upcoming solar conjunction.

9. Conclusions

The analysis of the range-rate residuals from four superior solar conjunctions reveals a relatively consistent pattern in how the Doppler noise varies with SEP angle. Certainly the accumulated amount of data is now sufficient to give a good indication of how range-rate measurements should be weighted for orbit determination purposes during future solar conjunctions.

A qualification concerns the possible influence of the noise level on the phasing within the 11 years solar cycle. 2006 coincided with the minimum so also the 2004 MEX solar conjunction was not far from minimum. The data from the VEX solar conjunction appears to show a correlation between short-term, high solar

activity (sunspot development, flares and coronal mass ejections) and higher than expected noise levels throughout either parts of or the whole of individual station passes.

The increase in Doppler noise begins already at an SEP angle above $10°$. When this angle has fallen to about $1°$ the rms noise on 2-way range-rate reaches 5 - 10 mm/s which is approaching a level two orders of magnitude larger than is usual at large SEP angles. Among future ESA missions, these results are most relevant for Bepi Colombo since Mercury spends 20% of each synodic period beyond the Sun, as seen from Earth, with an SEP angle below $10°$.

For Rosetta, no significant variation was observed in the noise on the range data throughout the solar conjunction period. The bias on the range data was substantially lower than expected from the nominal solar corona model hitherto used within the orbit determination software. A distinct, but also lower than expected, bias of about 4 mm/s magnitude was seen on the range-rate data on two days when the SEP angle was just $0.70°$. This bias is small compared with the peak-to-peak noise on the same days but very large compared with typical range-rate noise.

Using a suitable set-up for the orbit determination, an adjusted solar corona model was derived by estimating the two coefficients. This model and corresponding electron density estimates have been compared with the results from radio science investigations of other missions at solar conjunction. Although there is a wide variation between all the results, there is some evidence for a dependency on solar activity: the Rosetta data were obtained close to the minimum of the solar cycle and yield relatively low electron density estimates. Since the spacecraft stays in heliocentric orbit for many years, similar analyses at future solar conjunctions will cover the whole period between the extremes of solar activity.

With the estimation capability for the solar corona model parameters it may be possible to achieve a modest improvement in orbit determination accuracy during solar conjunction periods. A substantial improvement is impossible due to the high Doppler noise. If for a future mission like Bepi Colombo, using range and Doppler tracking data, it is desired to have navigation accuracies during solar conjunctions commensurate with those outside of conjunctions, then it is necessary to calibrate precisely the solar corona effects. This can be achieved only with simultaneous dual-frequency up- and downlink signals.

10. References

1. http://www.spaceweather.com/.

2. Moyer, T. D.: “Formulation for Observed and Computed Values of Deep Space Network Data Types for Navigation”, Monograph 2, Deep Space Communications and Navigation Series, JPL 00-7, 2000.

3. Muhleman, D. O., Esposito, P. B. & Anderson, J. D.: “The Electron Density Profile of the Outer Corona and the Interplanetary Medium from Mariner-6 and Mariner-7 Time-Delay Measurements”, Astrophysical Journal, 211, pp. 943-957, 1977 February 1.

4. Muhleman, D. O. & Anderson, J. D.: “Solar Wind Electron Densities from Viking Dual-Frequency Radio Measurements”, Astrophysical Journal, 247, pp. 1093-1101, 1981 August 1.

5. Newhall, X. X., Standish Jnr., E. M. & Williams, J. G.: “DE102: A numerically integrated ephemeris of the Moon and planets spanning forty-four centuries”, Astron. Astrophys., Vol. 125, pp. 150-167, 1983.

6. Ho, C. & Morabito, D.: “Solar Corona and Solar Wind Effects”, DSMS Telecommunications Link Design Handbook, 810-005, Rev. E, 106, Rev. A, NASA/DSN, 2005 October 21.

7. Bird, M. K. *et al*.: “The Coronal Electron Density Distribution Determined from Dual-Frequency Ranging Measurements During the 1991 Solar Conjunction of the Ulysses Spacecraft”, Astrophysical Journal, 426, pp. 373-381, 1994 May 1.